Lumped-Capacity Method for Easy Estimation of Interfacial Heat Transfer Coefficients in Die Casting

Zehui Sun, Guoli Li, Zhe Qian, Weifei Li, and Jian Jing

***Abstract*—The interfacial heat transfer coefficients (IHTCs) are the key parameters in numerical simulations on casting processes, but the inverse estimation of them from experiments is very difficult to be conducted and involves considerable uncertainty. With the assumptions of isothermal casting and one-dimensional heat conduction, this paper presents a lumped-capacity method for inverse estimation of IHTCs for die casting of high thermal conductivity metals. This method greatly simplifies the procedure of temperature measurements while providing estimation of IHTCs with reasonable accuracy.**

***Index Terms*—Interfacial heat transfer coefficient, high thermal conductivity casting, lumped-capacity method, one-dimensional heat conduction model.**

I. Introduction

The mechanical and electrical properties of a cast metal part may deviate greatly from the standard corresponding properties declared for this kind of metal. This is because the properties of a cast part heavily depend on the particular casting process from which the cast part is produced [1]. Thus, designing controlled casting processes that produce cast parts with desired properties is of great importance.

However, the detailed correlation between the process parameters and the thermal history of the castings is unknown for a new casting design. Trial-and-error experimental studies are very expensive and time consuming and hence, numerical simulations on casting processes are routinely carried out during a new casting design. The effectiveness of the numerical simulations primarily depends on the accuracy of the provided boundary conditions, among which the IHTCs are very difficult to be accurately determined, and thus comprise the main uncertainties in the numerical simulations [2].

Two main approaches are available to estimate IHTCs. One approach uses thermal contact models to estimate the IHTCs [3], [4], in which an equivalent air gap between the casting and the mold is assumed to arise from both surface roughness and thermal contract. The other approach estimates the IHTCs from inverse heat conduction analysis [5].

Inverse heat conduction analysis involves measuring transient temperatures at an array of appropriate positions and then solving an ill-posed problem to obtain the time-varying heat fluxes across the interface. The temperature measurement is the most difficult task in an inverse heat conduction study of die casting process. Due to the fast solidification rate in high pressure die casting (HPDC) process, the thermocouples' response time and their improper installations may introduce significant uncertainties into the estimations of IHTCs [2].

In the present paper, we propose a simple method in which only the temperature histories of castings are needed to estimate IHTCs and thus, can dramatically simplify the procedure of temperature measurements.

Manuscript received January 25, 2020; revised June 1, 2020.

Zehui Sun is with the Anhui University, China (e-mail: zhsun@ahu.edu.cn).

II. Heat Transfer in the Mold

For a cast metal of high thermal conductivity, e.g. most non-ferrous metals, the internal temperature field is nearly uniform. Hence, we can consider the temperature gradient only in the mold during thermal modeling. Moreover, the following features are present in die casting of a non-ferrous metal of high thermal conductivity. First, the surface of the cast part can be assumed as an isothermal surface, of which the temperature remains the melting point during solidification; second, the temperature gradient near the casting-mold interface in the mold are perpendicular to the interface; third, on solidification completing , the latent heat released into the mold usually has not reached the outer boundary of the mold, or even if it has, the heat conduction in the mold may not be affected significantly by the outer boundary conditions and thus, is still at the non-regular stage.

Given the above discussions, the heat conduction in the mold during casting solidification can be assumed as a one-dimensional conduction in a semi-infinite medium. If the casting-mold contact is perfect, this conduction problem is stated as (1) and (2),

$$\frac{\partial \theta}{\partial t} = a \frac{1}{r^n} \frac{\partial}{\partial r}\left(r^n \frac{\partial \theta}{\partial r}\right), \tag{1}$$

$$\theta(r,0) = 0, \quad \theta(r_w,t) = \theta_w \tag{2}$$

where r is the coordinate, a is the thermal diffusivity, and $\theta(r,t)$ is the temperature rise or shortly the temperature. Here, n=0, 1, 2 stands for cartesian, cylindrical and spherical coordinate, respectively.

For the problem (1) under the condition (2), the exact solutions for cartesian and spherical coordinates have already been obtained and presented in closed forms, while that for cylindrical coordinate is presented in an unsolved integral form [6]. However, the heat conduction into the mold during HPDC is essentially a short-time process, as discussed above, we may use the small-time asymptotic solution for the problem in cylindrical coordinate, which was given by Jaeger [6]. We summarize in Table A-I in Appendix

doi: 10.18178/ijmmm.2020.8.3.491

the existing solutions of the dimensionless heat fluxes across the boundaries of semi-infinite media, defined as

$$q^* = qL_c/(\lambda\theta_w)$$

where q is the heat flux, L_c is the characteristic length, and λ is the thermal conductivity. For more comprehensive review, one can refer to [7].

If a casting is hollow or it has an interior surface profile, then it requires a core. The thermal contact between the casting and the core should also be accounted for. The core is often of small size, and the heat released into it soon spreads across its whole volume. Thus, the heat conduction into the core cannot be viewed as that into a semi-infinite medium. For a non-ferrous casting with high thermal conductivity, we can still assume one-dimensional heat conduction in the core, as we have done for the heat conduction in the mold.

The solutions of heat conduction in finite volumes with simple geometries are generally presented in the forms of infinite series. For the Fourier number $Fo \geq 0.2$, one-term approximations of these solutions can be used, while $Fo < 0.2$, fitted approximations of the form as given in (3) are adopted.

$$q^*(Fo) = \frac{1}{\sqrt{\pi Fo}} + q^*_{ss}(Fo), \quad Fo < 0.2 \tag{3}$$

where $q^*_{ss}(Fo)$ is undetermined function and will be obtained by fitting (3) to the corresponding series. Both the fitted q^* for $Fo < 0.2$ and one-term approximate q^* for $Fo \geq 0.2$ are summarized in Table A-I, and more detailed review are provided in [7].

To represent the thermal conductance of the heat conduction into a body across its surface, we can define an equivalent heat transfer coefficient as

$$h_e = q^*\lambda/L_c \tag{4}$$

Further, we can calculate the accumulative heat transfer as

$$Q^*(Fo) = \int_0^{Fo} q^*(Fo')dFo' \tag{5}$$

of which the results are summarized in Table A-II in the Appendix.

In the following section, we will use (4) and (5) to construct the lumped-capacity heat balance equation for the solidification process of a high thermal conductivity casting.

III. Model for Latent Heat Dissipation

A. Heat Balance Equation of Solidification

When only the solidification process is concerned for thermal modeling, the heat balance equation of a high thermal conductivity casting can be simplified due to the features of the heat transfer process as discussed above.

The latent heat released from the molten casting equals the heat conducting across the mold surface into its volume, hence we have

$$\rho V \cdot H_s = \sum\nolimits_j A_j \int_0^{t_s} \theta_{wj}(t) h_{ej}(t) dt \tag{6}$$

where $\theta_{wj}(t)$ is the temperature of the mold contacting surface j; A_j is the surface area; and $h_{ej}(t)$, as defined in (4), is the equivalent thermal conductance related to the heat conduction in the mold.

Due to the interfacial thermal resistance, there exists a difference between $\theta_{wj}(t)$ and θ_m, denoted by $\Delta\theta_j(t)$ in (7) as

$$\vartheta_m = \theta_{wj}(t) + \Delta\theta_j(t) \tag{7}$$

Because the transient values of $\theta_{wj}(t)$ and $\Delta\theta_j(t)$ are all unknown, the integration in (6) cannot be performed.

We assume a constant IHTC denoted as $\bar{h}$ when addressing the interfacial thermal resistance. Then, it is pertinent to calculate the average values of $\theta_{wj}(t)$ and $\Delta\theta_j(t)$, respectively, as

$$\bar{\theta}_w = \frac{\sum_j A_j \int_0^{t_s} \theta_{wj}(t) h_{ej}(t) dt}{\sum_j A_j \int_0^{t_s} h_{ej}(t) dt}$$
$$\Delta\bar{\theta} = \frac{\sum_j A_j \int_0^{t_s} \theta_{wj}(t) h_{ej}(t) dt}{\bar{h}\, t_s \sum_j A_j} \tag{8}$$

Using $\bar{\theta}_w$ and $\Delta\bar{\theta}$ instead of $\theta_{wj}(t)$ and $\Delta\theta_j(t)$ in (7), we have

$$\bar{\theta}_w = \frac{\theta_m}{1 + \left(\sum_j A_j \int_0^{t_s} h_{ej}(t) dt\right) / \left(\bar{h} t \sum_j A_j\right)} \tag{9}$$

At this point, we can simplify the heat balance equation (6) by replacing $\theta_{wj}(t)$ with $\bar{\theta}_w$, and get

$$V \cdot H_s = \frac{\theta_m}{1 + \left(\sum_j A_j \int_0^{t_s} h_{ej}(t) dt\right) / \left(\bar{h} t_s \sum_j A_j\right)} \cdot \rho \sum_j A_j \int_0^{t_s} h_{ej}(t) dt \tag{10}$$

The equivalent heat conductance $h_{ej}(t)$ in (10) can be determined using (4) and (5), which yields

$$\sum\nolimits_j C_{cj} \cdot Q^*_j\left(\frac{a_j}{L_{cj}^2} t_s\right) = \frac{A\bar{h} t_s E_s/\Delta T}{A\bar{h} t_s - E_s/\Delta T} \tag{11}$$

where

$$C_{cj} = \rho c_p A_j L_{cj}, \quad E_s = \rho V H_s \tag{12}$$

By the heat balance equation for the solidification process, $\bar{h}$ can be inversely determined provided that t_s has been identified from the measured cooling curve of the casting.

The specific heat balance equations for casings of simple geometry are provided in the subsection B of Appendix.

Commonly, we are confronted with much complex casting shapes in practice. As an example, we consider HPDC of the copper rotor cage of an induction motor. A complex shape may be approximated by a combination of simple shapes. The assumed shapes for the interfaces between the rotor cage and its mold are summarized in Table A-III.

The rotor cage is composed of bars and end rings which are of different shapes and dimensions and contact with the mold zones of very distinct heat capacities. Consequently, the rotor bars and the end rings will solidify within very different periods of time. Here, we consider the solidification

process of the rotor bars and that of the end rings separately. The heat balance equation for the rotor bars and the end rings are provided in the subsection C in Appendix.

B. Time-Varying IHTC

The IHTC determined from (11), namely $\bar{h}$, is actually the one both spatially and temporally averaged. More often, the spatially-averaged but time-varying IHTC, denoted by $h(t)$, is of interest for numerical simulations on the casting thermal history.

A time-varying IHTC features a profile of which the rapidly decreasing portion occurring at the stage of solidification, followed by a stable portion after the solidification being completed. For simplicity, we simplify this profile into the one with a linear decreasing portion followed by a constant steady portion. Consequently, if the steady value of IHTC, denoted as h_{st}, is determined, the time-varying IHTC can be written as follows

$$h(t) = \begin{cases} 2\bar{h}(1 - t/t_s) + 2h_{st}(t/t_s - 1/2), & t \le t_s \\ h_{st}, & t > t_s \end{cases} \quad (13)$$

where h_{st} can be determined as follows

$$h_{st} = \frac{\sum_j A_j h_{ej}(t_s)/A - \bar{h}}{\bar{h}\sum_j A_j h_{ej}(t_s)/A}$$

or in terms of q_j^* as

$$h_{st} = \frac{\sum_j A_j q_j^*(t_s)/AL_{cj} - \bar{h}/\lambda_m}{\bar{h}\sum_j A_j q_j^*(t_s)/AL_{cj}}$$

The present IHTC estimation method only requires experimentally measured cooling curve of the casting, and the temperature gradient involving temperature measurements in an array of positions in the mold near the interface is not needed. Hence, this method greatly reduces the most difficult task in the inverse estimation of IHTCs.

IV. Numerical Validation

To validate the proposed method, finite element method (FEM) simulations are carried out on the heat dissipation processes of molten cast parts.

As far as numerical simulations are concerned, realistic profiles of IHTC, $h(t)$, are necessary interface conditions, unlike in the experimental tests. However, the rapidly varying profiles of $h(t)$ as well as the corresponding time intervals $0 < t \le t_s$ are all unknown.

Here we apply a constant IHTC, $\bar{h}$, in the numerical simulation models. From the obtained cooling curve, we can identify the solidification time t_s and solve for the IHTC from the relevant heat-balance equation. The calculated IHTC is then compared to the originally specified one.

TABLE I: Dimensions of the Rotor(mm)

Parameter	Symbol	values
Rotor radius	R_r	66
Rotor core length	l_r	120
Rotor yoke radius	R_y	44.5
Inner radius of end ring	R_{er}	38
Thickness of end ring	δ_{er}	17
Thickness of tooth	δ_t	2.9
Number of rotor bars	N_b	70

TABLE II: Thermal Properties of the Materials

	Copper		H13 Steel	
Parameter	Symbol	Value	Symbol	Value
Density (kg/m³)	ρ	8450	ρ_m	7700
Specific heat (kg·K)	c_p	495	c_{pm}	460
Thermal conductivity W/(m·K)	λ	334	λ_m	30
Latent heat (J/kg)	H_s	205000	—	—

The geometries of the castings considered here include an infinite plate, an infinite hollow cylinder, a spherical shell and a rotor cage. The plate has a thickness of $2\delta = 6mm$. The outer and inner radii of the hollow cylinder are chosen to be the same as those of the spherical shell, respectively, with the values $R_o = 10\text{mm}$, $R_i = 6\text{mm}$. The dimensions of the rotor cage are tabulated in Table I. The thermal properties of the casting material copper and the mold material H13 steel are supplied in Table II.

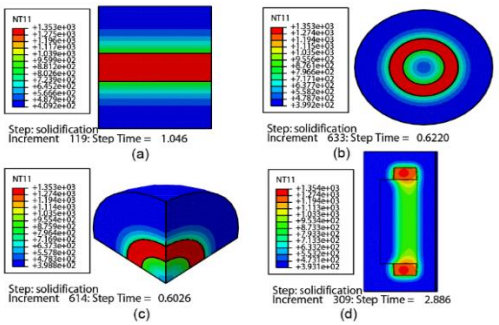

Fig. 1. Temperature contours of the casings on solidification completing: (a) infinite plate, (b) infinite hollow cylinder, (c) spherical shell and (d) rotor cage.

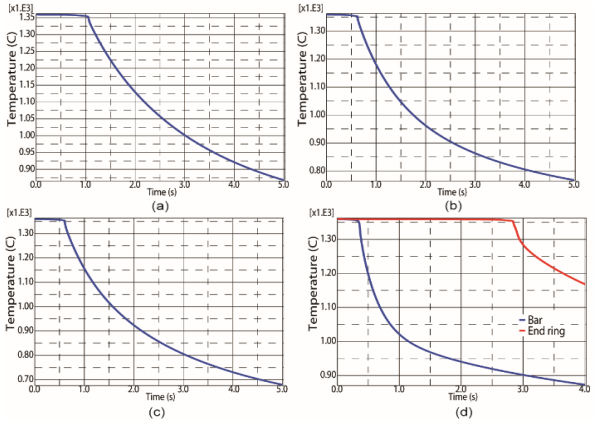

Fig. 2. The cooling curves of the castings: (a) infinite plate, (b) infinite hollow cylinder, (c) spherical shell, and (d) rotor cage.

We perform the FEM simulations using ABAQUS. The transient temperature contours of the cast parts are given in Fig. 1 for the moments when the maximum temperatures in the castings drop to the solidus temperature of copper, which indicates that the solidification of the corresponding casting has just completed. In the other hand, the cooling curves of these castings from the numerical simulations are plotted in Fig. 2. The solidification time of each casting can also be easily identified from the quite distinct constant regime of the cooling curve. Moreover, the solidification time identified from the cooling curve is essentially identical to that determined from the corresponding transient temperature field. Thus, it can be concluded that the solidification time of a high thermal conductivity casing can be determined from its measured cooling curve with reasonable certainty.

TABLE III: RESULTS FOR t_s(S) AND $\bar{h}$(104 W/(M·K))

Casting	t_s	$\bar{h}^{(a}$	$\bar{h}^{(b}$
Infinite plate	1.046	1.0	0.957
Hollow cylinder	0.622	1.0	0.968
Spherical shell	0.603	1.0	0.908
Rotor bars	0.356	1.0	0.812
Rotor end rings	2.886	1.0	1.139

a) Exact IHTC values; b) Calculated IHTC values.

Using the heat-balance equations given in Appendix, we compute the average IHTC for each cast part, and then compare it to its exact value specified as the interface condition for the corresponding FEM model. As shown in Table III, the calculated IHTCs are in reasonable agreement with their exact values.

The relatively large discrepancies occur in the cases of the rotor bars and the rotor end rings, which can be attributed to the approximations introduced into the heat-balance equations. However, the approximations in the heat-balance models can be identified and improved by the results of numerical simulations.

V. CONCLUSION

This paper presents a simple lumped-capacity method for inverse estimation of IHTCs in die casting. With this method, only the temperature history of the cast metal needs to be measured in the experiment, and the temperature gradient at the casting-mold interface is not needed for the estimation of the IHTC. Hence, the difficulties in the procedure of temperature measurements, together with the uncertainties involved, are greatly reduced.

The major approximations in this method arise from the simplifications made in the derivation of the balance equations for complex castings. But this type approximations can be identified and improved by numerical simulations.

It should be noted that the present method is only applicable for die casting of non-ferrous cast metals that generally have very high thermal conductivities.

APPENDIX

A. Solutions for Heat Transfer across Simple Boundaries

The analytical solutions to the heat fluxes across boundaries of simple geometries are summarized in Table A-I, while the corresponding solutions to the accumulative heat transfer are tabulated in Table A-II.

TABLE A-I: HEAT FLUX ACROSS BOUNDARY

Boundary Geometry	Semi-infinite media	Finite volume	
		Fo < 0.2	Fo ≥ 0.2
Planar	$1/\sqrt{\pi Fo}$	$1/\sqrt{\pi Fo}$	$2e^{-\frac{\pi^2 Fo}{4}}$
Cylindrical	$\frac{1}{\sqrt{\pi Fo}}+\frac{1}{2}-\frac{1}{4\sqrt{\pi}}\sqrt{Fo}+\frac{1}{8}Fo$	$\frac{1}{\sqrt{\pi Fo}}-\frac{1}{2}-\frac{3}{5}Fo$	$2e^{-\beta_1 Fo}$
Spherical	$1/\sqrt{\pi Fo}+1$	$1/\sqrt{\pi Fo}-1$	$2e^{-\pi^2 Fo}$

TABLE A-II: ACCUMULATIVE HEAT TRANSFER ACROSS UNIT BOUNDARY AREA

Boundary geometries	Mould	Core	
		Fo < 0.2	Fo ≥ 0.2
Planar	$2\sqrt{Fo}/\sqrt{\pi}$	$2\sqrt{Fo}/\sqrt{\pi}$	$1+\frac{8}{\pi^2}e^{-\frac{\pi^2}{4}Fo}$
Cylindrical	$2\frac{\sqrt{Fo}}{\sqrt{\pi}}+\frac{1}{2}Fo-\frac{Fo^{3/2}}{6\sqrt{\pi}}+\frac{1}{16}Fo^2$	$2\frac{\sqrt{Fo}}{\sqrt{\pi}}-\frac{1}{2}Fo-\frac{3}{10}Fo^2$	$\frac{1}{2}+\frac{2}{\beta_1^2}e^{-\beta_1^2 Fo}$
Spherical	$2\sqrt{Fo}/\sqrt{\pi}+Fo$	$2\sqrt{Fo}/\sqrt{\pi}-Fo$	$\frac{1}{3}+\frac{2}{\pi^2}e^{-\pi^2 Fo}$

B. Heat-Balance Equations for Solidification of Simple Castings

1) Infinite plate casting of thickness 2δ

$$\frac{\bar{h}t\,E_s/\Delta T}{\bar{h}t-E_s/\Delta T}=C_c\frac{2}{\sqrt{\pi}}\sqrt{a\,t},$$

where $E_s=2\rho\delta H_s$, $\quad C_c=\rho c_p$

2) Cast parts separated by infinite plate core of thickness 2δ

$$\frac{\bar{h}t\,E_s/\Delta T}{\bar{h}t-E_s/\Delta T}=C_c\frac{2}{\sqrt{\pi}}\frac{\sqrt{at}}{\delta},$$

where $C_c=\rho c_p\delta$

3) Hollow cylinder casting

For $Fo\leq 0.2$

$$\frac{A\bar{h}t_s\,E_s/\Delta T}{A\bar{h}t_s-E_s/\Delta T}=$$
$$C_{co}\left[\frac{2}{\sqrt{\pi}}\left(\frac{at}{R_o^2}\right)^{1/2}+\frac{1}{2}\frac{at}{R_o^2}-\frac{1}{6\sqrt{\pi}}\left(\frac{at}{R_o^2}\right)^{3/2}+\frac{1}{16}\left(\frac{at}{R_o^2}\right)^2\right]+$$
$$C_{ci}\left[\frac{2}{\sqrt{\pi}}\left(\frac{at}{R_i^2}\right)^{1/2}-\frac{1}{2}\frac{at}{R_i^2}-\frac{3}{10}\left(\frac{at}{R_i^2}\right)^2\right]$$

for $Fo>0.2$

$$\frac{A\bar{h}t_s\,E_s/\Delta T}{A\bar{h}t_s-E_s/\Delta T}=$$
$$C_{co}\left[\frac{2}{\sqrt{\pi}}\left(\frac{at}{R_o^2}\right)^{1/2}+\frac{1}{2}\frac{at}{R_o^2}-\frac{1}{6\sqrt{\pi}}\left(\frac{at}{R_o^2}\right)^{3/2}+\frac{1}{16}\left(\frac{at}{R_o^2}\right)^2\right]+C_{ci}\left(\frac{1}{2}+\frac{2}{\beta_1^2}e^{-\beta_1^2 at/R_i^2}\right)$$

where

$$E_s=\pi(R_o^2-R_i^2)\rho H_s,\qquad C_{co}=\rho_m c_{pm}\cdot 2\pi R_o^2,$$
$$C_{ci}=\rho_m c_{pm}\cdot 2\pi R_i^2\,,\qquad A=2\pi(R_o+R_i)$$

4) Spherical shell casting

For $Fo\leq 0.2$

$$\frac{A\bar{h}t_s\,E_s/\Delta T}{A\bar{h}t_s-E_s/\Delta T}=$$
$$C_{co}\left[2\left(\frac{at}{\pi R_o^2}\right)^{1/2}+\frac{at}{R_o^2}\right]+C_{ci}\left[2\left(\frac{at}{\pi R_i^2}\right)^{1/2}-\frac{at}{R_i^2}\right]$$

for $Fo>0.2$

$$\frac{A\bar{h}t_s\,E_s/\Delta T}{A\bar{h}t_s - E_s/\Delta T} = C_{co}\left[2\left(\frac{at}{\pi R_o^2}\right)^{1/2} + \frac{at}{R_o^2}\right] + C_{ci}\left(\frac{1}{3} + \frac{2}{\pi^2}e^{-\pi^2 at/R_i}\right)$$

where

$$E_s = 4\pi\left(R_o^3 - R_i^3\right)\rho\, H_s/3\ , \qquad C_{co} = 4\pi R_o^3 \rho_m c_{pm}\ ,$$
$$C_{ci} = 4\pi R_i^3 \rho_m c_{pm}$$

C. Heat-Balance Equations for Solidification of Cast Rotor Cage

1) Rotor bar

$$\frac{A\bar{h}t_s\,E_s/\Delta T}{A\bar{h}t_s - E_s/\Delta T} \approx C_c\left(1 + \frac{8}{\pi^2}e^{-\pi^2 at/\delta_t^2}\right)$$

where

$$E_s = \left[\pi\left(R_r^2 - R_y^2\right) - N_b\delta_t\left(R_r - R_y\right)\right]\rho H_s,$$
$$A \approx 2N_b\left(R_r - R_y\right), \qquad C_c = \rho_m c_{pm} A\,\delta_t\ /2$$

2) Rotor end ring

$$\frac{A\bar{h}t_s\,E_s/\Delta T}{A\bar{h}t_s - E_s/\Delta T} \approx C_c\left[2\left(\frac{at}{A_{er}}\right)^{1/2} + \frac{\pi}{2}\frac{at}{A_{er}} - \frac{\pi}{6}\left(\frac{at}{A_{er}}\right)^{3/2} + \frac{\pi^2}{16}\left(\frac{at}{A_{er}}\right)^2\right]$$

where

$$A_{er} = (R_r - R_{er})\delta_{er}, \qquad E_s = \rho c_p \pi A_{er}(R_r + R_{er})$$
$$A \approx [(R_r - R_{er}) + 2\delta_{er}]\cdot\pi(R_r + R_{er}) + \left(R_y - R_{er}\right)\cdot 2\pi R_{er},$$
$$C_c \approx \rho_m c_{pm} A\cdot\sqrt{A_{er}/\pi}$$

TABLE A-III: ASSUMED SHAPES FOR ROTOR CAGE AND MOLD INTERFACES

Casting-mold interface	Bar-Tooth	Bars-Yoke	Bars-Mod	End ring-Mold
Assumed shape	Infinite plane	Cylinder interior	Cylinder exterior	Cylinder exterior

CONFLICT OF INTEREST

The authors declare no conflict of interest.

AUTHOR CONTRIBUTIONS

A conducted the mathematical analysis and computation, and wrote the paper; B designed the work and supervised the entire research project; C helped with reviewing and providing suggestions to the work; D and E contribute to the finite element simulations. All the authors had approved the final version of the manuscript for publication.

ACKNOWLEDGEMENTS

This work was supported by the National Key R&D Program of China under Grant 2018YFB0104900.

REFERENCES

[1] E. Karakulak, "A review: Past, present and future of grain refining of magnesium castings," *Journal of Magnesium and Alloys*, vol. 7, no. 3, pp. 355-369, Sep. 2019.
[2] G. Dour, M. Dargusch, and C. Davidson, "Recommendations and guidelines for the performance of accurate heat transfer measurements in rapid forming processes," *International Journal of Heat and Mass Transfer*, vol. 49, no. 11–12, pp. 1773-1789, June 2006.
[3] A. Hamasaiid, G. Dour, T. Loulou, and M. Dargusch, "A predictive model for the evolution of the thermal conductance at the casting-die interfaces in high pressure die casting," *International Journal of Thermal Sciences*, vol. 49, no. 2, pp. 365-372, Feb. 2010
[4] A. Hamasaiid, M. S. Dargusch, T. Loulou, and G. Dour, "A predictive model for the thermal contact resistance at liquid–solid interfaces: Analytical developments and validation," *International Journal of Thermal Sciences*, vol. 50, no. 8, pp. 1445-1459, Aug. 2011.
[5] J. V. Beck, "Nonlinear estimation applied to the nonlinear inverse heat conduction problem," *International Journal of Heat and Mass Transfer*, vol. 13, no. 4, pp. 703-716, April 1970.
[6] H. S. Carslaw and J. C. Jaeger, *Conduction of Heat in Solids*, 2nd ed. Oxford: Claremore Press, 1959
[7] A. S. Lavine and T. L. Bergman, "Small and large time solutions for surface temperature, surface heat flux, and energy input in transient, one-dimensional conduction," *J. Heat Transfer*, vol. 130, no. 10, pp. 101302, Oct. 2008.

Zehui Sun received the B.S. degree in civil engineering from Hefei University of Technology, Hefei, China, in 2000, and the Ph.D. degree in modern mechanics from University of Science and Technology of China (USTC), Hefei, in 2007. From 2007 to 2013, he worked as a postdoctoral fellow with USTC. Since 2013, he has been a lecturer with Anhui University, Hefei. His researches focus on thermal analysis and optimization of electric machines and power electronics.

Guoli Li received the B.S. and M.S. degrees in electrical engineering from the Hefei University of Technology, Hefei, China, in 1983 and 1987, respectively, and the Ph.D. degree in nuclear energy science and engineering from the Hefei Institute of Physical Sciences, Chinese Academy of Sciences, Hefei, in 2006. From 2007 to 2010, she was a professor with the Zhejiang University of Technology, Hangzhou, China. Since 2010, she has been a professor with Anhui University, Hefei. Her research interests include motor optimization and robotics.

Zhe Qian received his Ph.D. degree in power electronics and power transmission from Hefei University of Technology, Hefei, China, in 2012. Since 2012, he has been a lecturer with Anhui University, Hefei. His research interests include the special motors and their control systems.

Weifei Li received the B.S. degree in electrical engineering from West Anhui University, Luan, China, in 2018. He is currently working toward the M.S. degree at the College of Electrical Engineering and Automation, Anhui University, Hefei, China. His research interest includes thermal analysis of electric machines and power electronics.

Jian Jing received the B.S. degree in electrical engineering from Harbin University of Science and Technology, Harbin, China, in 2018. He is currently working toward the M.S. degree at the College of Electrical Engineering and Automation, Anhui University, Hefei, China. His research interest includes thermal analysis of electric machines and power electronics.